Research Article

Development and characterization of a novel hydrogel dressing for co-delivery of resveratrol and gallic acid via cyclodextrin inclusion complexation for wound healing

Khin Cho Aye, Supusson Pengnam, Boonnada Pamornpathomkul, Thapakorn Charoenying, Prasopchai Patrojanasophon, Praneet Opanasopit, and Chaiyakarn Pornpitchanarong

DOI: 10.34172/PS.025.43171

To appear in: Pharmaceutical Science (https://ps.tbzmed.ac.ir/)

Received date: 10 Sep 2025

Revised date: 12 Nov 2025

Accepted date: 9 Dec 2025

Please cite this article as: Aye KC, Pengnam S, Pamornpathomkul B, Charoenying T, Patrojanasophon P, Opanasopit P. Development and characterization of a novel hydrogel dressing for co-delivery of resveratrol and gallic acid via cyclodextrin inclusion complexation for wound healing. Pharm Sci. 2026. doi: 10.34172/PS.025.423171

Development and characterization of a novel hydrogel dressing for co-delivery of resveratrol and gallic acid via cyclodextrin inclusion complexation for wound healing

Khin Cho Aye[1https://orcid.org/0009-0003-3869-7077], Supusson Pengnam[1,2], Boonnada Pamornpathomkul[1,2], Thapakorn Charoenying[1,2], Prasopchai Patrojanasophon[1,2], Praneet Opanasopit[1,2,*] https://orcid.org/0000-0002-4878-2529, and Chaiyakarn Pornpitchanarong[1,2,*] https://orcid.org/0000-0001-6540-280X

[1] Pharmaceutical Development of Green Innovations Group (PDGIG), Faculty of Pharmacy, Silpakorn University, Nakhon Pathom, 73000, Thailand

[2] Research and Innovation Center for Advanced Therapy Medicinal Products, Faculty of Pharmacy, Silpakorn University, Nakhon Pathom 73000, Thailand

***Corresponding author:**

Chaiyakarn Pornpitchanarong, Ph.D.

Department of Industrial Pharmacy, Faculty of Pharmacy,

Silpakorn University, Nakhon Pathom, Thailand 73000

Email: pornpitchanaron_c@su.ac.th

Tel: +66-34-255800 Fax: +66-34-250941

Abstract

Background: The therapeutic potential of polyphenols like resveratrol (Res) and gallic acid (GA) in wound healing is limited by their poor aqueous solubility and chemical instability. This study aimed to develop and characterize a novel hydrogel-based drug delivery system to overcome these limitations and achieve synergistic therapeutic effects. **Methods:** The strategy involved two key components, a Res/GA inclusion complex (Res/GA-IC) prepared using hydroxypropyl-β-cyclodextrin (HP-β-CD) to enhance polyphenol solubility and stability, and a dual-crosslinked carboxymethyl cellulose-poly(vinyl alcohol) (CMC-PVA) hydrogel formulated as a delivery vehicle for the IC. The properties of the Res/GA-IC and the final hydrogel patch were characterized. **Results:** Formulation of the Res/GA-IC resulted in a remarkable increase in the

aqueous solubility of Res. The Res/GA combination showed strong synergistic antioxidant activity (CI < 0.3), and the Res/GA-IC demonstrated enhanced antibacterial efficacy against Staphylococcus aureus. The CMC-PVA hydrogel dressing incorporating the IC showed favorable physicochemical properties, including appropriate swelling capacity, structural integrity, and sustained release characteristics for both active agents. Crucially, the final formulation was highly biocompatible with human fibroblast cells. **Conclusion:** This work presented a successful formulation strategy for the co-delivery of poorly soluble synergistic polyphenols. The developed hydrogel dressing represents a promising therapeutic platform for advanced wound management by effectively addressing key challenges of oxidative stress and bacterial infection.

Key words: Resveratrol; gallic acid; inclusion complex; hydrogel; wound healing

1. Introduction

Wounds are a significant health concern, often referred to as a "silent epidemic" due to their substantial social and economic burden on millions of people.[1] While acute wounds typically heal on their own in healthy individuals, chronic wounds present a major challenge due to complications such as infection, insufficient angiogenesis, and excessive oxidative stress which delay healing process. This issue is particularly pronounced as the population ages and the incidence of obesity, diabetes, and vascular disease increases.[2] The global wound care market is projected to grow at a compound annual growth rate (CAGR), reaching USD 30.52 billion by 2030, up from USD 20.18 billion in 2022.[3] This highlights the urgent need for advanced wound dressings that surpass traditional bandages to facilitate faster, more efficient healing.

Among these, hydrogel dressings have emerged as a significant advancement in wound care, offering a moist environment that accelerates healing while enhancing patient comfort. Their unique physicochemical properties make them particularly effective in managing both acute and chronic wounds.[4] Hydrogels are three-dimensional polymeric networks with a hydrophilic, porous structure that enables substantial water or biological fluids absorption, often exceeding several times their dry weight. Their hydrophilicity stems from cross-linked polar functional groups such as amide, amino, carboxyl, and hydroxyl moieties. Formed via physical or chemical crosslinking of natural or synthetic polymers, hydrogels exhibit tunable mechanical properties, degradation rates, and bioadhesiveness.[5] Beyond maintaining moisture, hydrogels function as drug delivery platforms, facilitating controlled release of therapeutic agents, including antibiotics, growth factors, and herbal drugs.[6] This dual functionality accelerates healing by mitigating infections, modulating inflammation, and promoting tissue regeneration, positioning hydrogels as a highly promising class of advanced wound dressings.[7]

Polyvinyl alcohol (PVA) and carboxymethyl cellulose (CMC) are widely used for hydrogel formation due to their biocompatibility, biodegradability, and ability to form stable networks.[8] PVA provides excellent film-forming ability and chemical resistance, while CMC enhances water absorption and introduces functional groups for crosslinking.[9, 10] These polymers can be crosslinked physically through freeze-thaw cycles, which induce PVA crystallization and create microcrystalline domains, and chemically using metal ions to form ionic interactions and coordination complexes.[11] Zhang et al. reported that physically crosslinked cellulose/PVA hydrogels exhibited superior mechanical strength and elasticity, whereas chemically crosslinked hydrogels showed higher swelling but reduced strength. Combining both methods can balance mechanical properties and water retention.[12]

Naturally derived bioactive compounds like polyphenols, flavonoids, and alkaloids offer antioxidant, anti-inflammatory, and antimicrobial effects.[13] Resveratrol (Res), a stilbene-class polyphenol, supports tissue repair by reducing oxidative stress and inflammation, and shows synergistic antioxidant activity with compounds like catechin, caffeic acid, and curcumin.[14, 15] Gallic acid (GA), a phenolic acid found in plants such as palm leaves, also exhibits strong antioxidant and antimicrobial activity, particularly against *Pseudomonas aeruginosa* and *Staphylococcus aureus* biofilms.[16, 17] While both Res and GA have known antioxidant properties, their combined effects remain underexplored. However, Res's poor solubility and GA's instability limit their therapeutic use. Inclusion complexes (ICs) with cyclodextrins, especially hydroxypropyl beta-cyclodextrin (HP-β-CD), can improve solubility, stability, and bioavailability, and are well-suited for hydrogel incorporation. Although the antioxidant activity of Res and GA are widely described, there is limited information about their interactions and potential synergistic or antagonistic effects.[18, 19] Incorporating quercetin–HP-β-CD ICs into PVA hydrogels enhanced antioxidant activity and wound healing, supporting the potential of such systems.[20, 21]

This study aimed to develop a dual-crosslinked PVA–CMC hydrogel incorporating Res/GA inclusion complexes (Res/GA-IC) with hydroxypropyl-β-cyclodextrin (HP-β-CD). While inclusion complexes with HP-β-CD are an established method for improving polyphenol solubility, the specific innovation of this work is the co-encapsulation of a synergistic Res/GA combination. This study quantitatively demonstrated the synergistic antioxidant and antibacterial interactions of this specific polyphenol pairing. We hypothesized that integrating this optimized Res/GA-IC into a dual-crosslinked hydrogel scaffold would create a multifunctional dressing with significant, synergistic potential for wound healing applications by simultaneously addressing oxidative stress and infection. This work advances the field by demonstrating the quantitative synergy of Res and GA within a hydrogel scaffold, applying HP-β-CD co-encapsulation, and integrating these complexes into a dual-crosslinked PVA–CMC hydrogel to achieve simultaneous infection control, oxidative stress mitigation, and cytocompatibility.

2. Materials and Methods

2.1. Materials

Res and GA (purity ≥99%) were obtained from Sigma-Aldrich® (St. Louis, MO, USA), while HP-β-CD (CAVASOL W7 HP PHARMA) was supplied by Maxway Co., Ltd. Other reagents, including CMC, PVA, 2,2-diphenyl-1-picrylhydrazyl (DPPH), methyl-thiazolyl diphenyl tetrazolium bromide (MTT), and dimethyl sulfoxide (DMSO), were also purchased from Sigma-Aldrich®. High-performance liquid chromatography (HPLC) grade acetonitrile and methanol were sourced from Merck & Co. (Darmstadt, Germany). Cell

culture reagents, including penicillin-streptomycin, fetal bovine serum (FBS), and Dulbecco's Modified Eagle's Medium (DMEM), were procured from Gibco BRL (Rockville, MD, USA). Normal human skin fibroblast (NHF) cells were obtained from the American Type Culture Collection (ATCC, Rockville, MD, USA). All chemicals and reagents used in this study were of analytical grade.

2.2. Preparation of Res/GA-HP-β-CD inclusion complex

The ICs of Res, GA, and the Res/GA combination with HP-β-CD were prepared using the co-evaporation method.[18] Initially, HP-β-CD was dissolved in distilled water at various molar ratios relative to Res or GA (2:1, 1:1, and 1:2) to form a clear aqueous solution. Res or GA was dissolved in methanol, and the methanolic Res or GA solution was gradually added to the aqueous HP-β-CD solution under continuous stirring. The mixture was stirred overnight in a sealed glass container to ensure thorough encapsulation of Res or GA within the HP-β-CD cavity. After encapsulation, the resulting clear solution was centrifuged to remove any unencapsulated Res or GA. The supernatant was then subjected to solvent removal using a rotary evaporator at 40 °C under reduced pressure, yielding a paste-like inclusion complex. This paste was lyophilized to obtain a dry powder, which was stored in an airtight container until further analysis. Moreover, the synergy ratio of Res and GA was encapsulated in a HP-β-CD, following the same protocol.

2.3. Characterization of Res/GA-HP-β-CD inclusion complex

The chemical interactions in the inclusion complexes were analyzed using an attenuated total reflection Fourier-transform infrared (ATR-FTIR) spectrometer (Nicolet iS5, Thermo Fisher Scientific, MA, USA). The spectra were recorded over a scanning range of 4000 to 500 cm^{-1} with a resolution of 4 cm^{-1}. The samples were directly placed on the ATR crystal for the analysis without further preparation.

2.4. Determination of antioxidant activity using DPPH assay

The DPPH free radical scavenging activity was assessed based on a previously reported method with modifications.[22] Freshly prepared 0.2 mM DPPH solution and various concentrations of sample solutions were prepared in methanol. In a 96-well microplate, 100 µL of the DPPH solution was mixed with 100 µL of sample solution at concentrations ranging from 3.125–100 µg for Res and 0.625–20 µg for GA. For the control, 200 µL of the DPPH solution in methanol was used. The reaction mixture was incubated in the dark for 20 min, after which the absorbance was measured at 550 nm using a multimode microplate reader (VICTOR Nivo™, PerkinElmer, Germany). The percentage of DPPH free radical

scavenging activity was calculated using Eq. 1, and IC50 values were determined through linear regression analysis.

$$\%\text{DPPH scavenging} = \frac{A_{control} - A_{sample}}{A_{control}} \quad (1)$$

2.5. Combination Index Analysis

The synergistic ratios of Res and GA binary mixtures on the antioxidant activity were evaluated using the Chou-Talalay method.[23] This method, based on the median-effect equation derived from the law of mass action, provides a comprehensive framework for analyzing the interactions of individual and combined agents. Drug combinations were quantitatively assessed through the combination index (CI) theorem, which classifies interactions as additive (CI = 1), synergistic (CI < 1), or antagonistic (CI > 1). The analysis was performed using CompuSyn software (version 1.0) for precise calculation and interpretation.

2.6. Determination of water solubility and complexation efficiency of the inclusion complexes

To determine the water solubility of Res, GA, and their inclusion complexes, approximately 100 mg of each sample was suspended in 5 mL of water and mixed at 25 °C for 72 h. The suspensions were then centrifuged at 11,000 rpm for 15 min to remove any insoluble materials. The amounts of Res and GA in the supernatant were analyzed using an Agilent 1220 Infinity II HPLC system (Agilent Technologies, Santa Clara, USA). The samples were diluted in methanol, filtered through a 0.45-µm nylon filter, and injected into the HPLC system. The HPLC conditions were adapted from previous studies with slight modifications.[24, 25] For Res, the chromatographic separation was performed on a C18 column (4.6 × 250 mm, 5 µm) with a flow rate of 1 mL/min, using a mobile phase of 0.1% v/v acetic acid in water and acetonitrile (70:30), and detection at 306 nm. For GA, a C18 column (4.6 × 150 mm, 5 µm) was used with a mobile phase of methanol and 0.01% v/v ortho-phosphoric acid in water (90:10, pH adjusted to 3), with detection at 272 nm. Additionally, the encapsulation of Res and GA within the HP-β-CD cavity was evaluated using a direct approach. In this method, 55 mg of Res-IC, GA-IC, and Res/GA-IC were dissolved in 5 mL of methanol and analyzed using the same HPLC procedure. The concentrations were determined based on the predetermined calibration curves for Res and GA, and the complexation efficiency (%CE) was calculated using the Eq. 2.

$$\%CE = \frac{\text{Amount of entrapped Res or GA}}{\text{Initial amount loaded in the HP-β-CD}} \times 100 \quad (2)$$

2.7. Antibacterial activity

The antibacterial activity of Res, GA, Res-IC, GA-IC, and Res/GA-IC against *S. aureus* was evaluated using the broth microdilution method. All test samples were dissolved in tryptic soy broth (TSB), and two-fold serial dilutions were prepared in a 48-well plate, ranging from 100 – 3200 µg/mL for Res and 37.5 – 1200 µg/mL for GA. Each well was inoculated with 3 µL of fresh sub-cultured bacterial suspension (10^6 CFU/mL) and incubated at 37 °C for 24 h. The MIC was determined as the lowest concentration with no visible bacterial growth. To determine the MBC, 10 µL from wells showing no visible growth were plated onto tryptic soy agar (TSA) and incubated at 37 °C for 24 h. The MBC was recorded as the lowest concentration that resulted in no bacterial growth.

2.8. Preparation of Res/GA-IC loaded hydrogel patch

To prepare the Res/GA-IC-loaded hydrogel patch, PVA and CMC solutions were prepared separately and then mixed at a 2:1 weight ratio, resulting in a total polymer weight of 1.05 g in a 10 g hydrogel formulation. A citric acid solution (10% w/w of the CMC weight) was added dropwise to the polymer mixture, followed by 0.1% DAAA (dihydroxy aluminum amino acetate) dissolved in 5% glycerol. A total of 50 mg of the Res/GA-IC, containing 3.5 mg of Res and 2.5 mg of GA, was incorporated into 10 g of the polymer mixture and stirred for 1 h until a homogeneous blend was achieved. This amount was selected based on their synergistic antioxidant activity and to ensure a therapeutically relevant dose for localized wound healing.[26, 27] The prepared hydrogel solution (10 g) was poured into a rectangular mold measuring 35 × 60 mm with a thickness of 5 mm. A freeze-thaw process was conducted to facilitate double crosslinking by freezing the hydrogel at -20 °C for 18 h, followed by thawing at 25 °C for 6 h, repeated for three cycles. The hydrogel was gently rinsed with water three times to remove any unloaded inclusion complex or non-crosslinked components and then stored at 2–8 °C, protected from light, for further analysis.

2.9. Physical characterization of Res/GA-IC loaded hydrogel patch

2.9.1. Swelling behavior

The swelling behavior of the Res/GA-IC-loaded hydrogel patch was evaluated to determine its fluid uptake capacity. The measurement was performed using a gravimetrical method. Approximately weight 1.5 g of both the Res/GA-IC-loaded hydrogel and the blank hydrogel were first dehydrated in an oven at 50 °C until they reached a constant equilibrium weight. The dried hydrogels were weighed and then fully immersed in 10 mL of phosphate buffer solution (PBS) pH 7.4 at 37 °C. After 12 h of immersion, the swollen hydrogels were carefully removed from the medium, and any excess water on their surfaces

was gently wiped off. The weight of the swollen hydrogels was recorded. The percentage of fluid uptake was calculated using the Eq. 3.

$$\text{Fluid uptake } (\%) = \frac{W_s - W_d}{W_d} \times 100 \quad (3)$$

Where, W_s is the weight of swollen hydrogel and W_d is the weight of dried hydrogel

2.9.2. Water content

The water content of the hydrogels was determined by measuring the initial weight and the dry weight of the hydrogels. Briefly, the hydrogels were accurately weighed in their initial state, then dried in an oven until a constant weight was achieved. The water content was calculated using the Eq. 4.

$$\text{Water content } (\%) = \frac{W_i - W_d}{W_d} \times 100 \quad (4)$$

Where, W_i and W_d are the weight of hydrogel in its initial state and dry state, respectively.

2.9.3. Gel content

The gel content of the hydrogels was analyzed to verify the crosslinking density between the polymer chains in the hydrogel matrix. Initially, the hydrogel samples were dried in an oven (50°C) until a constant weight was obtained. The dried hydrogels were then immersed in 10 mL of deionized water for 24 h. After swelling, the hydrogels were dried once more under same conditions, and their final dry weights were measured. The percent of gel content was computed by the Eq. 5.

$$\text{Gel content } (\%) = \frac{W_{d1} - W_{d2}}{W_{d1}} \times 100 \quad (5)$$

Where, W_{d1} and W_{d2} represent the initial and final dried weight of hydrogel.

2.9.4. Mechanical strength

The compressive mechanical test was also conducted using a texture analyzer (TA. XT Plus, Stable Micro Systems, Godalming, UK) to verify the mechanical stability of the hydrogel under compressive forces. The hydrogel samples (12 × 12 cm) were cut and compressed with a 5-mm stainless steel ball probe attached to the analyzer. The probe was lowered at a speed of 2 mm/s, applying pressure to the hydrogel until it ruptured. The force required to deform the hydrogel was measured, and its compressive toughness was determined using Eq. 6.

$$\text{Compressive toughness} = \frac{\text{Maximum force at breaking point}}{\text{Area of hydrogel exposed to compression}} \quad (6)$$

2.9.5. Morphology

The morphology of the hydrogels was analyzed using a scanning electron microscope (SEM; Tescan Mira3, Brno, Czech Republic) to observe the structural features of lyophilized swollen hydrogels, simulating their native state in fluid. A small piece of hydrogel was carefully cut transversely from the central region using a sharp blade. The specimen was mounted on an aluminum stub using conductive adhesive tape and sputter-coated with a thin layer of gold. SEM images were captured at an accelerating voltage of 5 kV.

2.10. Loading capacity and entrapment efficiency of Res/GA-IC in the hydrogel patch

HPLC analysis was conducted to quantify the total amount of Res and GA loaded in the hydrogel patch. Approximately 1.5 g of hydrogel samples were crushed and immersed in 30 mL of methanol within sealed bottles. The hydrogel fragments were agitated at 120 rpm for 4 h using an incubator shaker, followed by centrifugation at 12,000 rpm for 20 min to collect the extracted Res and GA. The resulting extract was diluted with methanol and filtered through a 0.45-µm nylon membrane filter before being analyzed using the HPLC methods detailed in section 2.6. The loading capacity (LC) and loading efficiency (%LE) were calculated using Eq. 7 and Eq. 8, respectively.

$$LC = \frac{\text{Quantified amount of Res or GA}}{\text{Weight of Res/GA-IC loaded hydrogel}} \quad (7)$$

$$\%EE = \frac{\text{Quantified amout of Res or GA}}{\text{Initial added amount of Res or GA}} \times 100 \quad (8)$$

2.11. Release study

The *in vitro* drug release from the hydrogel matrix was investigated. The release medium, composed of PBS (pH 7.4) containing methanol, was maintained under sink conditions. Hydrogel samples were immersed in 30 mL of the release medium and incubated at 37 °C with continuous shaking at 120 rpm using an incubating shaker. At specific time intervals, 1 mL of the medium was withdrawn for analysis and replaced with an equal volume of fresh medium to maintain a constant total volume. The collected samples were filtered through a 0.45 µm syringe filter to eliminate hydrogel residues and analyzed for drug concentration using HPLC. The cumulative release percentage was calculated by combining the drug released at each time point.

2.12. Cytotoxicity study

The MTT assay was performed to evaluate the cytotoxicity of the hydrogel samples. Hydrogel samples were sterilized by UV exposure for 30 min on each side and immersed in 5 mL of DMEM at 37 °C

for 6 h. The resulting extraction media, equivalent to concentrations of 8.75 µg/mL of Res and 6.25 µg/mL of GA, were collected and diluted in DMEM to prepare three two-fold serial dilutions. NHF cells were seeded at a density of 10,000 cells per well in DMEM supplemented with 10% FBS in a sterile 96-well culture plate and incubated until confluence. The medium was then replaced with 100 µL of the hydrogel extracts, and the cells were incubated at 37 °C with 5% CO_2 for 24 h. After incubation, 25 µL of freshly prepared MTT solution (1 mg/mL in PBS) was added to each well, followed by further incubation at 37 °C for 3 h. The medium was subsequently removed, and 100 µL of DMSO was added to dissolve the formazan crystals produced by viable cells. Absorbance was measured at 550 nm using a microplate reader. Cell viability was calculated as the ratio of the absorbance of each sample to that of the blank control.

2.13. Statistical analysis

All experiments were performed in triplicate, and the data are presented as the mean ± standard deviation. An independent two-tailed t-test was used to compare two groups. For comparisons among multiple groups, a one-way analysis of variance (ANOVA) followed by Tukey's post hoc test was conducted. Statistical analyses were carried out using SPSS® software version 19 (SPSS Inc., Chicago, IL, USA), with a significance threshold set at $p < 0.05$.

3. Results and discussion

3.1. Synergistic antioxidant activity of Res and GA combination

The antioxidant activities of Res and GA were assessed using the DPPH assay, revealing clear dose-dependent scavenging effects, as shown in **Figure 1(a)** and **1(b)**. Res showed moderate antioxidant activity, with approximately 52% inhibition at 28 µg/mL and an IC_{50} of 26.36 µg/mL. In contrast, GA exhibited significantly stronger activity, achieving 98% inhibition at just 5 µg/mL, with a much lower IC_{50} of 3.42 µg/mL. These results are in line with earlier reports and highlight GA's potent radical-scavenging ability.[28] The superior antioxidant capacity of GA is largely due to its molecular structure, which includes three adjacent hydroxyl groups on the aromatic ring. This arrangement allows GA to readily donate hydrogen atoms to neutralize free radicals and form resonance-stabilized phenoxy radicals. Additionally, the ortho-positioned hydroxyl groups enable intramolecular hydrogen bonding, further enhancing radical stability. Stoichiometric studies have shown that a single GA molecule can quench up to six DPPH radicals, emphasizing its strong electron-donating ability.[29] In comparison, Res has a stilbene-based structure with two hydroxyl groups on each aromatic ring. While it does offer some antioxidant activity through hydrogen donation and resonance stabilization, its lower hydroxyl density and less favorable configuration

limit its efficiency compared to GA.[30] These structural differences help explain the observed variation in activity and support the rationale for combining the two compounds to potentially achieve enhanced, synergistic antioxidant effects.

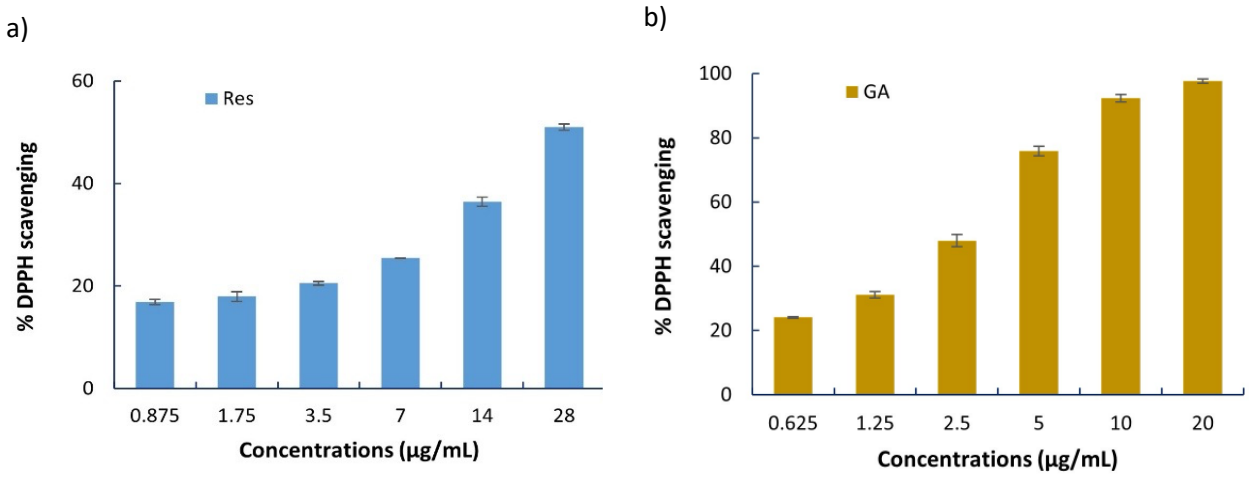

Figure 1. Percentage of DPPH scavenging activity of (a) Res; (b) GA at different concentrations.

Given their different antioxidant strengths, the combination of Res and GA was investigated for synergistic effects. Various fixed-ratio combinations (1.4:1 to 44.8:1) were evaluated using the DPPH assay, and the data were analyzed using the Chou-Talalay method via CompuSyn software. The software calculates the CI values, which quantitatively describes the nature of the interaction at different effect levels, expressed as the fraction affected (Fa) corresponding to 50%, 75%, and 95% inhibition (Fa = 0.5, 0.75, and 0.95).

The results, summarized in Table 1, identified the 1.4:1 (Res:GA) ratio as the most effective and synergistic combination. This ratio exhibited the strongest effect, with the lowest Dm (1.8763 µg/mL) and CI values indicating strong synergy (0.3831 at Fa = 0.5 and 0.2132 at Fa = 0.95). In contrast, as the proportion of Res increased, CI values rose, indicating a loss of synergy. This trend suggests that excessive Res may dilute the antioxidant contribution of GA or introduce competitive interactions possibly due to saturation of free radical binding sites that impair overall efficacy. The observed synergy is clearly ratio-dependent, with the most pronounced activity occurring when GA is present in a higher proportion. This enhanced effect is attributed to the complementary antioxidant mechanisms of Res and GA, when GA enables rapid neutralization of free radicals, Res contributes to radical stabilization through its π-conjugated stilbene backbone. Such synergistic behavior is consistent with previous reports, which

highlight that the combination of polyphenols can lead to improved antioxidant performance due to cooperative redox mechanisms, especially when their structures and reactivities are complementary [31]. This strong synergy at the 1.4:1 ratio was further supported by high drug reduction index (DRI) values for both Res (19.9) and GA (3.0). Based on these findings, the consistently low CI values (CI<0.3) across multiple effect levels, along with the lowest Dm value and favorable DRI values confirm that the 1.4:1 fixed ratio represents the most effective and synergistic combination [23]. The graphical outputs from this analysis (Figure 2) and a direct experimental comparison (Figure 3) visually confirm these findings, showing the combination is significantly more potent than the individual compounds or their additive effect.

Table 1. Medium-effect dose (Dm) and Combination index (CI) values at Fa = 0.5, 0.75, and 0.95 for various fixed-ratio combinations of Res and GA based on DPPH radical scavenging activity

Combination ratio (Res:GA)	**Dm (μg/mL)**	**CI@Fa=0.5**	**CI@Fa=0.75**	**CI@Fa=0.95**
1.4:1	1.8763	0.3831	0.2791	0.2132
2.8:1	3.4341	0.5291	0.8459	2.3621
5.6:1	5.4729	0.5395	0.8648	2.4681
11.2:1	8.9116	0.5704	1.0598	3.2413
22.4:1	12.6733	0.5641	1.0422	2.7734
44.8:1	16.1536	0.5513	1.3618	4.2469

CI value <0.1: very strong synergism; 0.1-0.3: strong synergism; 0.3-0.7: synergism; 0.7-0.85: moderate synergism; 0.85-9: slight synergism; 0.9-1.1: nearly additive; >1: antagonism.

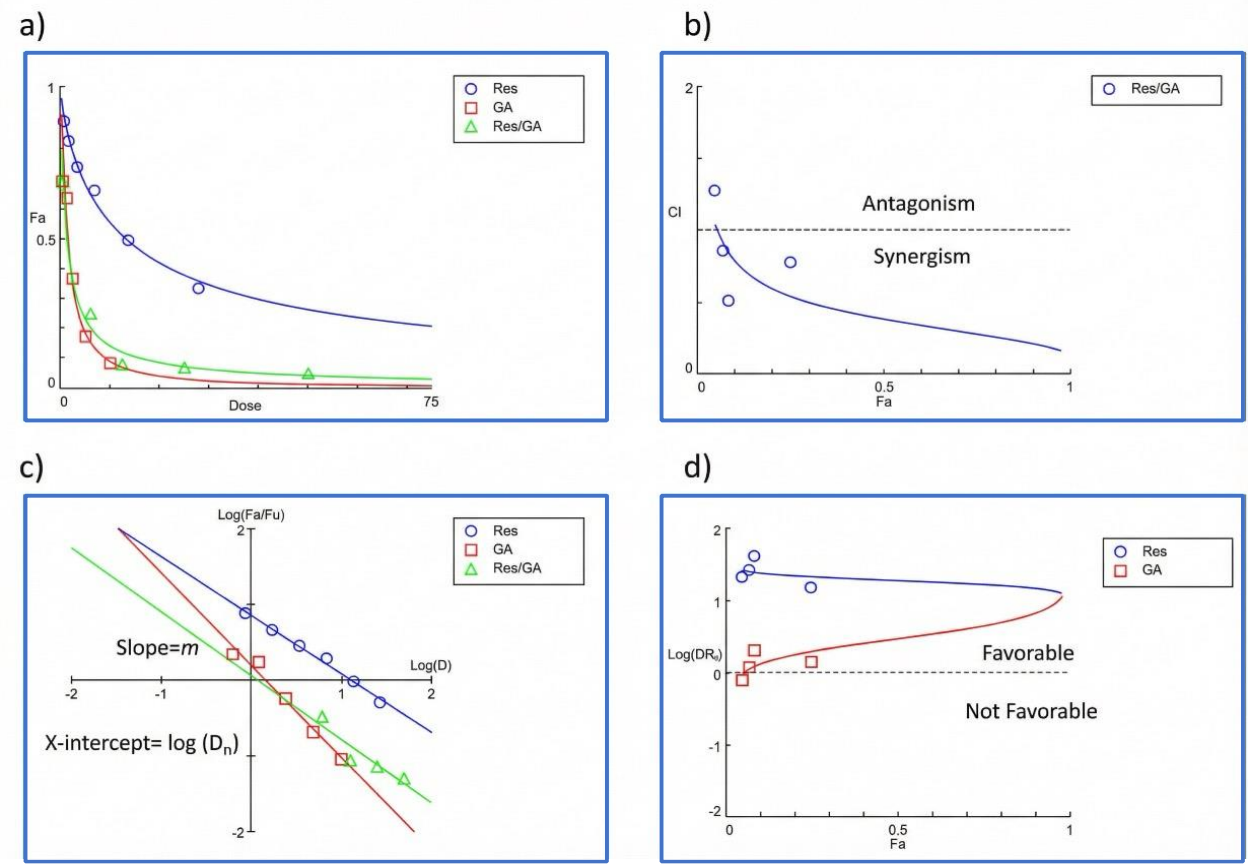

Figure 2. (**a**) Combination dose-effect curve of Res and GA interactions; (**b**) median-effect plot; (**c**) Fa-CI plot (Chou-Talalay Plot); and (**d**) Fa-DRI plot (Chou-Talalay Plot)

The experimental validation of this synergy is further supported by the DPPH scavenging results shown in **Figure 3**, where the antioxidant activity of selected combination (weight ratio 1.4:1 of Res to GA) is compared with that of each compound alone across various concentrations. At all tested doses, the combination consistently exhibited higher scavenging activity than either Res or GA individually. Notable, at the 3.5/2.5 µg/mL combination, the inhibition exceeded 60%, clearly surpassing the additive effect of the individual treatments. This enhanced performance aligns with the low CI values obtained from the CompuSyn analysis and reinforces the conclusion that the 1.4:1 ratio provides a synergistic advantage in free radical scavenging, making it an efficient and promising combination for further development.

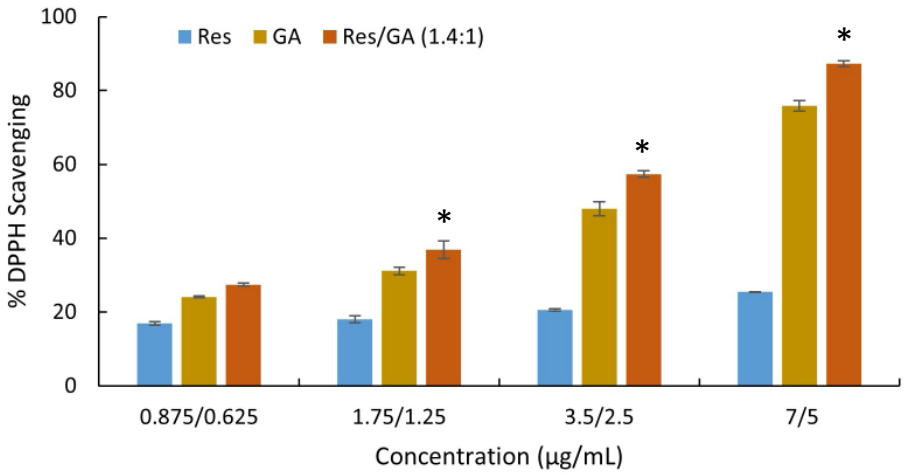

Figure 3. Synergistic antioxidant activity of Res/GA at a weight ratio of 1.4:1 compared to individual Res and GA. (* Significant difference compared to single Res and GA, $p<0.05$)

Despite their synergistic effects, the low aqueous solubility of Res and the oxidative susceptibility of GA presented challenges for bioavailability. Therefore, encapsulating the optimized Res-GA combination in HP-β-CD was pursued to improve solubility, stability, and sustained antioxidant activity. HP-β-CD is β-cyclodextrin derivative, with outer hydrophilic surfaces, and inner hydrophobic cavity. It has been shown to effectively encapsulate insoluble guest molecules within its hydrophobic cavities, enhancing their aqueous solubility by forming inclusion complexes.[32]

The formation of the Res/GA-HP-β-CD inclusion complex was confirmed through FTIR analysis, as shown in **Figure 4**. Res exhibited characteristic peaks around 1600 cm^{-1} (C=C stretching) and 3400 cm^{-1} (O–H stretching), while GA shows a strong C=O stretching peak near 1700 cm^{-1} and a broad O–H stretching band at 3200–3400 cm^{-1}, indicating the presence of functional groups in their pure forms. The spectrum of HP-β-CD displayed a broad O–H stretching band around 3400 cm^{-1}, indicative of multiple hydroxyl groups, as well as intense C–O–C stretching bands in the range of 1100–1000 cm^{-1}, characteristic of the glycosidic ether linkages in the cyclodextrin ring. The physical mixture closely resembles the HP-β-CD spectrum, with minimal changes in peak positions or intensities. This similarity suggested the absence of significant molecular interactions among the components. In contrast, the spectrum of the Res/GA-HP-β-CD inclusion complex (Res/GA-IC) demonstrated several notable alterations. In addition to the reduced intensity of the broad O–H stretching band and the suppression of the sharp C=O band at 1700 cm^{-1} (GA) and the C=C band at 1600 cm^{-1} (Res), significant changes were also observed in the spectral region

between 1300–1500 cm^{-1}. Specifically, the bands corresponding to aromatic skeletal vibrations and O–H bending modes, typically observed in this region, showed a marked decrease in intensity and partial overlapping with the HP-β-CD bands. The band near 1440–1460 cm^{-1}, often associated with aromatic C–H bending in Res and GA, was notably attenuated, or shifted in the inclusion complex spectrum. Additionally, the peak near 1370 cm^{-1}, attributed to O–H in-plane bending and phenolic group vibrations, became significantly broadened and less distinct. These changes suggested a modification of the local environment of the phenolic and aromatic functional groups, consistent with their encapsulation within the hydrophobic cavity of HP-β-CD. The observed spectral changes strongly support the successful formation of the Res/GA-HP-β-CD inclusion complex. The spectral evidence is indicative of reduced molecular freedom and altered hydrogen-bonding interactions as a result of host–guest complexation.

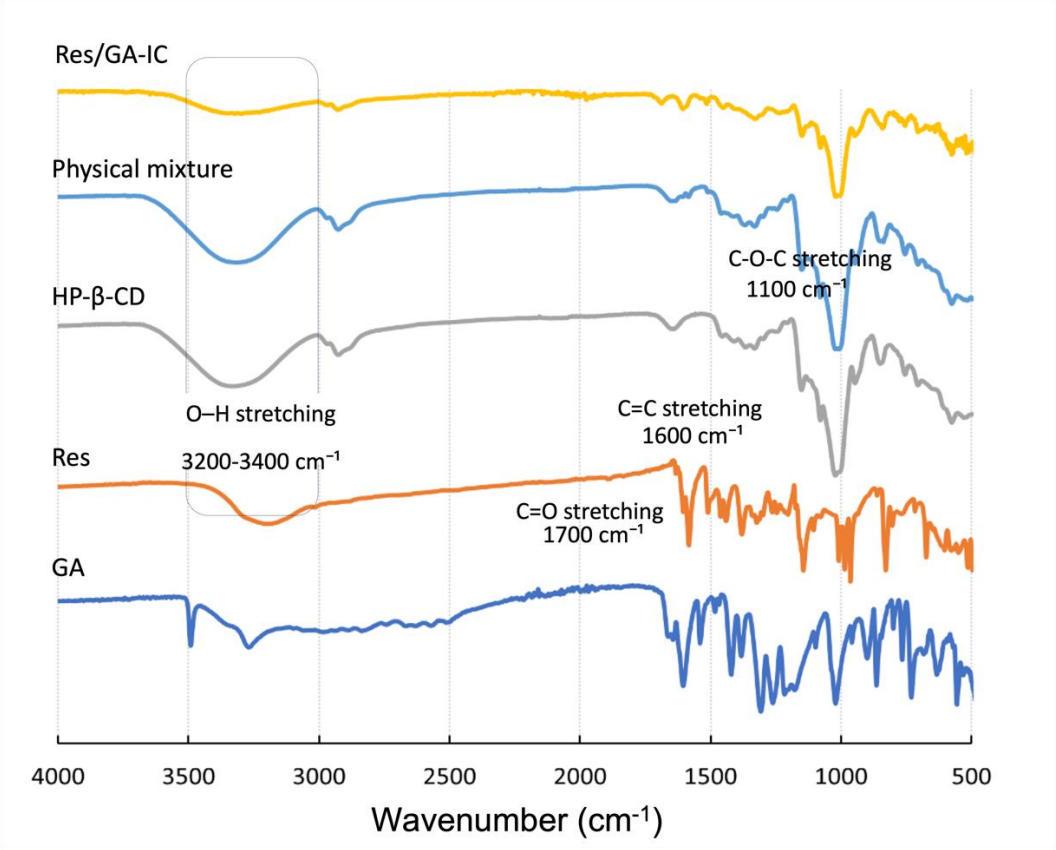

Figure 4. FTIR spectra of Res, GA, HP-β-CD, Res and GA physical mixture, and the Res/GA-IC

3.2. Complexation efficiency and water solubility

The CE and water solubility of Res and GA are key indicators of successful inclusion within the HP-β-CD cavity and presented in **Table 2**. Res was first complexed with HP-β-CD at varying molar ratios. The

1:1 and 1:2 molar ratios (Res:HP-β-CD) achieved near-complete complexation, with CE values of 100%, both significantly higher ($p < 0.05$) than the observed at a 2:1 ratio. These high CE values directly correlated with enhanced solubility which increased dramatically for over 300-fold ($p < 0.05$). GA also showed excellent inclusion behavior, achieving 100 % CE at a 1:2 GA: HP-β-CD ratio, with a significant solubility enhancement ($p < 0.05$). Notably, co-complexation of Res and GA in a 1:1:2 molar ratio (Res:GA: HP-β-CD) maintained high CE values for both compounds, while further improving their solubilities. Moreover, the 1:1:2 molar ratio (Res:GA: HP-β-CD) corresponds closely to the 1.4:1 weight ratio, making it a suitable and convenient choice for encapsulating the synergistic combination in HP-β-CD. These findings demonstrated that HP-β-CD not only enables efficient encapsulation of Res and GA, both individually and in combination, but also significantly enhances their aqueous solubility which is an essential factor for improving bioavailability in therapeutic applications.

The observed complexation efficiency and solubility enhancement of Res and GA upon inclusion with HP-β-CD underscore the suitability of HP-β-CD as a solubilizing agent for poorly water-soluble polyphenols. The nearly complete complexation at molar ratios of 1:1 and 1:2 (Res: HP-β-CD) suggests a favorable host–guest interaction, likely driven by hydrophobic interactions between the aromatic moiety of Res and the non-polar cavity of HP-β-CD. The successful co-complexation of Res and GA indicated that HP-β-CD can accommodate multiple guest molecules or form ternary complexes, potentially through non-covalent interactions such as hydrogen bonding or π–π stacking. These results are consistent with previous reports demonstrating efficient encapsulation of planar, hydrophobic molecules within cyclodextrin derivatives.[33, 34]

Notably, the co-complexation of Res and GA at a 1:1:2 molar ratio yielded high inclusion efficiency, indicating the feasibility of simultaneous incorporation of both compounds. This may involve the formation of a ternary complex or the presence of multiple binding interactions, including hydrogen bonding and van der Waals forces. The enhancement in aqueous solubility observed post-complexation particularly the approximately 327.76-fold increase in Res solubility emphasizes the profound impact of cyclodextrin inclusion on dissolution properties.[35] While GA exhibited a modest 1.92-fold solubility increase, likely because of its greater intrinsic hydrophilicity relative to Res, as well as potential differences in binding orientation or complex stability.[36] The dual improvement in solubility for both compounds suggest potential for co-delivery systems that may enhance their bioavailability and therapeutic outcomes.

The enhanced solubility of both compounds is particularly relevant to their application in wound healing formulations. Poor water solubility has traditionally limited the bioavailability and clinical

effectiveness of Res, despite its promising pharmacological profile. By increasing its solubility more than 300-fold, HP-β-CD inclusion may facilitate greater tissue penetration, sustained antioxidant action, and improved modulation of inflammatory pathways at the wound site.[37] Likewise, the increased solubility of GA may contribute to more effective scavenging of ROS, protection against oxidative stress, and support of cellular processes essential for wound repair.[38] Furthermore, the successful co-complexation of Res and GA in a single HP-β-CD system suggests the possibility of synergistic antioxidant effects, which could further enhance therapeutic outcomes in wound management. These findings confirmed HP-β-CD as an effective solubility-enhancing carrier for both compounds.

Table 2. Percentage of complexation efficiency (CE) and water solubility of Res and GA inclusion complexes at different molar ratio to HP-β-CD (Significant difference, $p<0.05$, (*) compared to Res-IC (2:1), (**) compared to the solubility of Res, ($^{\#}$) compared to the solubility of GA)

Samples	CE (%)	Water solubility (mg/mL)
Res	-	0.0631±0.001
Res-IC (2:1)	64.83±0.26	11.58±1.06
Res-IC (1:1)	100.87±0.33*	19.48±1.06**
Res-IC (1:2)	102.47±0.44*	19.42±0.17**
GA	-	8.33±0.18
GA-IC (1:2)	100.01±0.49	15.58±0.14#

3.3. Antioxidant activity of Res/GA-IC

To further evaluate the impact of complexation on antioxidant efficacy, the DPPH radical scavenging activity of Res, GA, and their 1.4:1 combination was assessed at defined concentrations, with the 1.4:1 ratio selected based on the synergistic antioxidant effect previously demonstrated in Section 3.1. As shown in **Figure 5**, Res (3.5 µg/mL) exhibited approximately 20% scavenging activity, which modestly increased to 26% after complexation. GA (2.5 µg/mL) showed a more notable improvement, rising from 48% to 63%. Most significantly, the Res/GA combination at 3.5/2.5 µg/mL demonstrated a synergistic scavenging effect, with scavenging activity increasing from 58% to over 74% post-complexation. These findings indicate that the complexation enhances the antioxidant activity of both individual components, with an even greater effect observed for their synergistic combination.

The enhanced antioxidant activity observed after complexation of Res, GA, and their synergistic blend (Res/GA-IC) can be attributed to improved solubility and molecular stability. Inclusion complexation

with cyclodextrin significantly enhances the aqueous solubility and dispersion of these poorly water-soluble polyphenols, increasing their effective concentration and promoting more efficient interaction with DPPH radicals.[39, 40] Additionally, the complexation provided a protective microenvironment that shields the sensitive hydroxyl groups of Res and GA from environmental degradation such as oxidation, UV exposure, or pH fluctuations, thereby preserving molecular integrity and sustaining antioxidant functionality throughout the assay.[34, 41] The synergistic Res/GA-IC holds substantial therapeutic promise for wound healing, where oxidative stress plays a pivotal pathological role. Its potent ROS-scavenging capability not only mitigates cellular damage but also promotes re-epithelialization and matrix remodeling.[42, 43] Importantly, the demonstrated synergy allowed effective antioxidant activity at lower doses, minimizing the risk of cytotoxicity or irritation, an essential advantage for topical applications.[44] Complexation improves the solubility, stability, and bio-efficacy of Res and GA, making the Res/GA-IC system a promising candidate for incorporation into hydrogels or other localized delivery platforms aimed at enhancing wound healing outcomes.

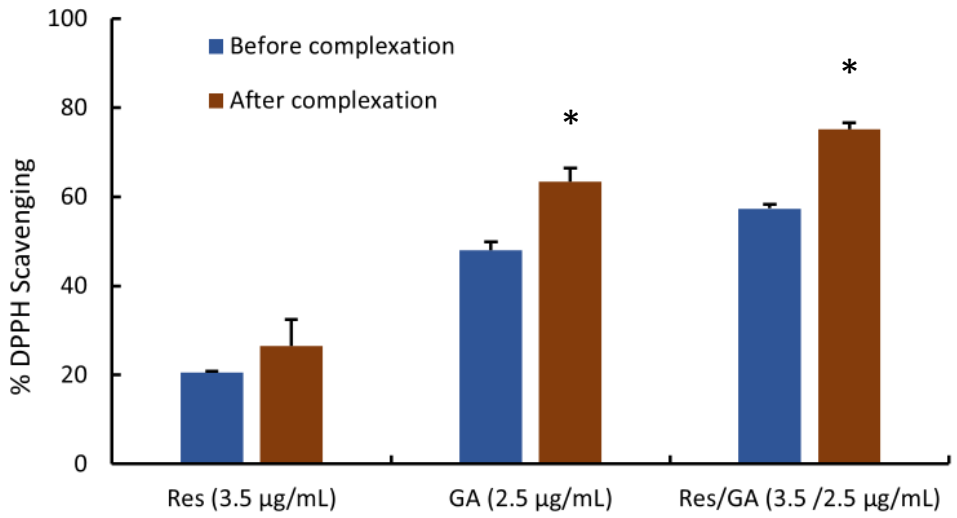

Figure 5. DPPH scavenging activity of RES, GA, and their synergistic combination before and after inclusion complex formation with HP-β-CD (*Significant difference compared to prior to complexation, $p<0.05$)

3.4. Antibacterial effect

The results in **Table 3** demonstrates that both Res and Res-IC exhibited no detectable antibacterial activity against *S. aureus*, with MIC and MBC values equal to or exceeding 2400 µg/mL. In contrast, GA demonstrated moderate antibacterial activity. Upon formation of the inclusion complex (GA-IC), GA's antibacterial potency was markedly enhanced, as evidenced by a two-fold reduction in both MIC and MBC

values. This improvement suggested increased efficacy following complexation. The most significant antibacterial activity was observed with the combined Res/GA-IC complex. These results indicated a clear synergistic interaction between Res and GA in the inclusion complex, resulting in a substantial enhancement of antibacterial activity compared to the individual or separately complexed compounds.

The observed synergistic antibacterial activity of the Res/GA-IC complex can be explained by the mechanisms reported for Res and GA. GA has been shown to induce intracellular reactive oxygen species (ROS), leading to oxidative damage of vital cellular components such as membranes, proteins, and nucleic acids.[45, 46] Res has been reported in the literature to act as a modulator of bacterial efflux pumps (e.g., NorA), thereby reducing the bacteria's ability to expel antimicrobial agents and detoxify intracellular ROS.[47] This was possibly the cause contributing to the lower MIC and MBC values observed for the Res/GA-IC complex. In addition, the amphiphilic nature of the Res–GA combination may facilitate membrane interactions, potentially improving permeability and intracellular delivery of both compounds.[48] The inclusion complexes also enhanced the aqueous solubility of Res and GA and enabled their co-delivery, which likely contributed to prolonged exposure and sustained antimicrobial pressure against the bacterial cells.[49] Together, these factors may help explain the synergistic antibacterial effect observed.

The demonstrated antibacterial synergy underscores the potential of the Res/GA-IC complex as an antimicrobial strategy, particularly in contexts such as infected wound management, where bacterial burden is a critical barrier to healing. By significantly lowering bacterial growth at reduced concentrations, the Res/GA-IC hydrogel could help create a more favorable microenvironment for tissue repair by reducing infection-driven inflammation. Moreover, both Res and GA possess additional wound-beneficial properties reported in the literature, including antioxidant, anti-inflammatory, and pro-angiogenic effects.[48, 50, 51] Although further *in vitro* and *in vivo* studies are needed to confirm these mechanisms and their relevance to wound healing, the present findings highlight the potential of the Res/GA-IC hydrogel as a promising candidate for future advanced wound care applications.

Table 3. MIC and MBC values of Res, GA, their inclusion complex, and combination inclusion complex against *S. aureus*

Samples	**MIC (μg/mL)**	**MBC (μg/mL)**
Res	>2400	>2400
Res-IC	>2400	>2400

GA	600	1200
GA-IC	300	600
Res/GA-IC	200/150	400/300

3.5. Formation and characterization of Res/GA-IC@ PVA-CMC hydrogel patch

In a macroscopic visual analysis, both PVA-CMC and Res/GA-IC@PVA-CMC hydrogels exhibited a white, opaque appearance with a smooth surface. The uniform polymer distribution indicated no phase separation or segregation, resulting in a flexible and durable hydrogel patch with a thickness of 5.5 ± 0.3 mm. The hydrogel formation was achieved through a combination of chemical and physical crosslinking mechanisms between PVA and CMC. PVA contributed to film-forming ability, while CMC enhanced hydrophilicity and water retention. Chemical crosslinking was primarily facilitated by citric acid, which promoted esterification between the hydroxyl (–OH) groups of the polymers and the carboxyl (–COOH) groups of citric acid.[52, 53] Additionally, Al^{3+} ions bridged multiple CMC chains via coordination complex formation,[54] further enhancing network stability. Physical crosslinking was achieved through a freeze-thaw process, inducing PVA crystallization, which led to the formation of microcrystalline domains acted as physical crosslinking points.[55] This synergistic dual-crosslinking approach significantly improved the hydrogel's mechanical strength, flexibility, and stability. To confirm hydrogel formation and successful crosslinking, the water content, gel content, and swelling percentage in PBS at pH 7.4 of hydrogels were investigated using a gravimetric method. These parameters are crucial in wound healing application. Water content maintains a moist environment, promoting cell migration and tissue regeneration. Gel content indicates crosslinking, affecting stability, degradation, and drug release. Swelling percentage regulates exudate absorption and moisture balance.[56] The incorporation of the Res/GA-IC into CMC-PVA hydrogels resulted in notable changes in their physicochemical properties presented in **Table 4**. The water content slightly decreased indicating the replacement of Res/GA-IC, thus the hydrogel retained its hydration capability. However, the significant decrease in gel content and the corresponding reduction in fluid absorption should be critically interpreted. While the values decreased, a final fluid absorption of 311.26% remains a highly favorable property for an advanced wound dressing. The clinical goal is to balance exudate absorption with maintaining a moist wound bed; an overly absorbent hydrogel (>500%) can risk dehydrating the wound, while low absorption can lead to maceration.[20, 57] Despite these changes, the compressive modulus remained relatively stable suggesting that the hydrogel maintained a promising

mechanical integrity. This compressive modulus of approximately 35 kPa is well within the established range for PVA-based hydrogels, which can be tuned from 24 kPa to over 2500 kPa depending on the formulation. More specifically, our value is directly comparable to other PVA/CMC hydrogels developed for wound healing, which have reported compressive strengths in the range of 65.5 kPa to 99.2 kPa. Our hydrogel's value on the softer side of this range is ideal for its intended application, confirming it is a soft, flexible matrix that can conform to the wound bed without causing irritation.[58, 59] The compressive modulus of a hydrogel is also vital for wound healing applications as it influences mechanical integrity, softness, and flexibility. A suitable modulus ensures the hydrogel can withstand mechanical stresses while conforming to the wound's shape, enhancing patient comfort.[60]

Table 4. Physicochemical properties of hydrogels

Hydrogels	PVA-CMC hydrogels	Res/GA-IC@PVA-CMC hydrogels	Literature value
Water content (%)	82.62±0.22	81.48±0.26	80-90%[61, 62]
Gel content (%)	79.53±1.65	59.51±3.24	> 50%[58]
Fluid absorption (%)	412.86±19.59	311.26±1.23	300-600%[63]
Mechanical strength (kPa)	35.18±1.26	34.38±1.07	30-100 kPa[58, 59]

The SEM images illustrated distinct microstructural differences between the hydrogels. As shown in **Figure 6(a-b),** the blank PVA-CMC hydrogel exhibited a well-defined, interconnected porous network with larger, uniform pores. This structure is known to facilitate fluid uptake and gel stability. In contrast, the Res/GA-IC-loaded PVA-CMC hydrogel **(Figure 6(c-d))** displayed a denser, more compact pore structure with smaller, irregular pores and a rougher surface morphology. These morphology changes are likely due to the incorporation of the Res/GA-IC. The presence of multiple -OH groups in Res and GA may initially contribute to increased network density through additional hydrogen bonding. However, unlike covalently crosslinked structures, these interactions are relatively weak and can be disrupted upon contact with water. This disruption loosens the hydrogel network, contributing to increased erosion. Moreover, the denser structure and smaller pores reduce fluid uptake, lowering the swelling capacity. This observation aligns with previous reports on polyphenol-loaded hydrogels, which exhibit reduced swelling due to tighter network packing but remain prone to gradual disintegration in aqueous environments because of dynamic, non-covalent interactions.[64] These structural findings are consistent with the physiological properties data discussed earlier, further confirming the impact of Res/GA-IC incorporation on the hydrogel's swelling and erosion behavior.

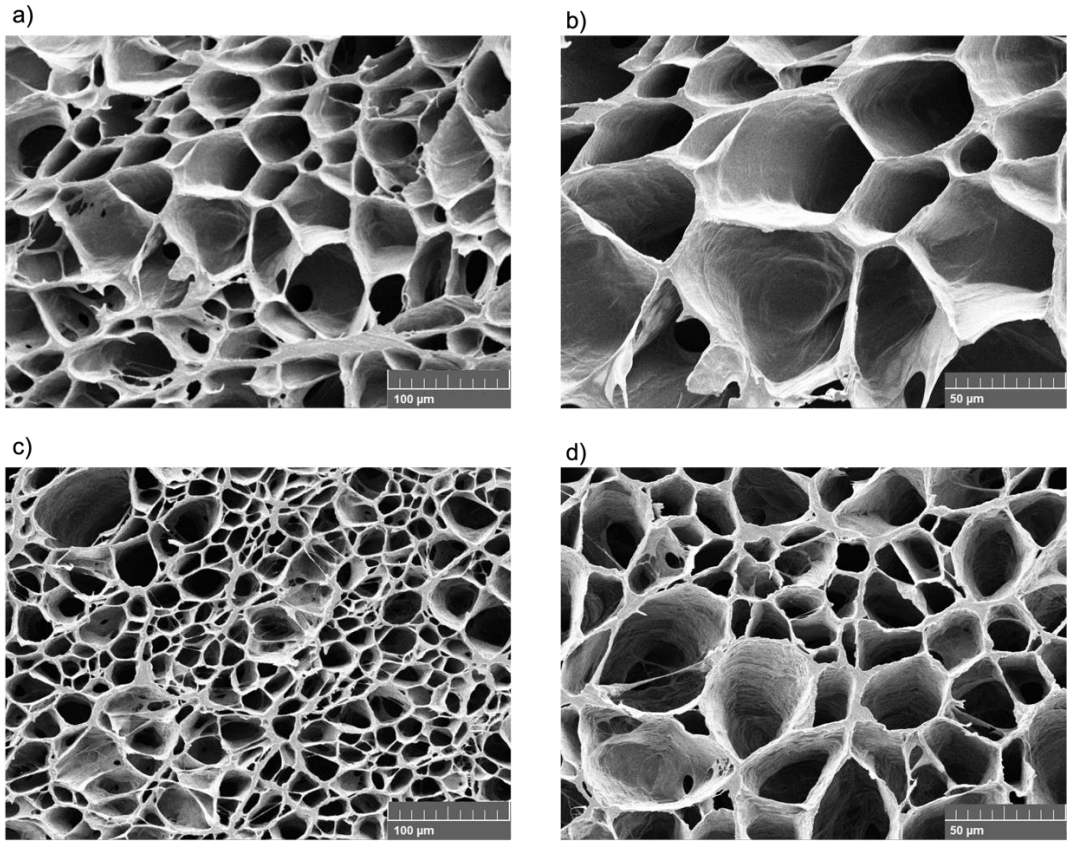

Figure 6. SEM images of (**a-b**) PVA-CMC hydrogel and (**c-d**) Res/GA-IC loaded PVA-CMC hydrogel in the swollen state at 500× and 1k× magnification

3.6. Drug content and release study

The Res/GA-IC was successfully incorporated into the PVA-CMC hydrogel, achieving high LC for both Res and GA. These loading levels align with therapeutically relevant ranges reported in previous studies; Zhang et al. and Kumar et al. demonstrated that Res and GA loadings in hydrogel systems were effective in promoting antioxidant and wound healing responses.[26, 27] EE were remarkably high for Res and GA **(Table 5)** indicating minimal loss during the fabrication process and strong retention within the hydrogel network. The *in vitro* release profile in PBS (pH 7.4), shown in **Figure 7**, exhibited a biphasic pattern: Res displayed an initial burst within the first few hours followed by a sustained release, reaching nearly 80% cumulative release at 24 h, while GA was released more gradually, reaching about 48% in the same period. Although co-encapsulated, the differing release behaviors likely stem from their distinct physicochemical properties. Res, being more hydrophobic, interacts weakly with the hydrophilic polymer network, facilitating faster diffusion. In contrast, GA's higher polarity and multiple hydroxyl groups

promote stronger interactions particularly with CMC's carboxyl and hydroxyl groups resulting in slower, more sustained release.[27, 65] Such controlled release is particularly beneficial in wound healing, as it helps maintain effective local drug concentrations, reduces dosing frequency, minimizes systemic exposure, and provides continuous antioxidant and anti-inflammatory effects.[66] Overall, this hydrogel system presents a promising platform for the localized and sustained delivery of natural bioactive compounds.

The 24-h study duration was intentionally selected to align with the intended clinical application. Given the hydrogel's high fluid absorption capacity (over 300% as shown in Table 4), it was designed for managing exudative wounds, which typically require daily dressing changes. This 24-h application cycle was necessary to manage exudate levels and maintain a clean wound environment. Therefore, the observed release profile, which delivered the therapeutic payload over 24 h, was ideal for this intended daily-wear application. Future *in vivo* studies will be used to confirm the optimal application frequency required for healing.

Table 5. Loading capacity and entrapment efficiency of Res/GA-IC in the hydrogel matrix

Res/GA@PVA-CMC hydrogels	LC (mg/g)	EE (%)
Res	0.34±0.01	98.99±1.09
GA	0.25±0.02	97.66±2.32

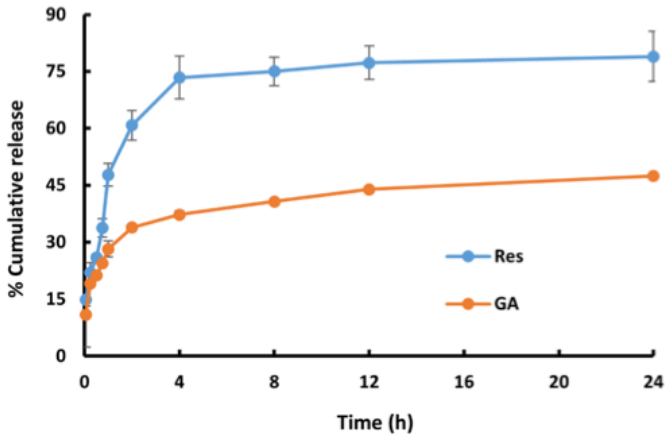

Figure 7. Percent cumulative release of Res and GA from the hydrogel matrix at pH 7.4

3.7. Cytotoxicity evaluation

The cytotoxicity of Res/GA-IC@PVA-CMC hydrogels was assessed using NHF cells to evaluate their safety for potential wound dressing applications. As shown in **Figure 8**, the MTT assay results revealed that cell viability remained above 100% at all tested hydrogel concentrations compared to the untreated control cultured in fresh DMEM. These concentrations correspond to Res/GA-IC contents equivalent to approximately 1.75/1.25 µg/mL, 3.5/2.5 µg/mL, and 7/5 µg/mL, respectively. This range was chosen to cover both effective and higher doses, ensuring a sufficient safety margin for the hydrogel system. The findings confirmed that the Res/GA-IC@hydrogels are non-toxic to NHF cells, even at elevated concentrations.

The enhanced solubility and bioavailability provided by the inclusion complex likely support efficient cellular uptake of Res and GA. Both compounds have been reported to protect cells from oxidative damage and promote the migration and proliferation of keratinocytes and fibroblast processes essential for wound repair.[67, 68] Additionally, the hydrogel matrix composed of PVA and CMC is known for its excellent biocompatibility and has been widely used in biomedical applications.[69] These polymers contribute to the hydrogel's non-cytotoxic profile, forming a moist and supportive environment for cell growth and tissue regeneration. Above all, the combination of biocompatible polymers and the Res/GA-IC in the hydrogel formulation supports safe interaction with human fibroblasts, highlighting its strong potential as a wound dressing that promotes healing while preserving cell viability.

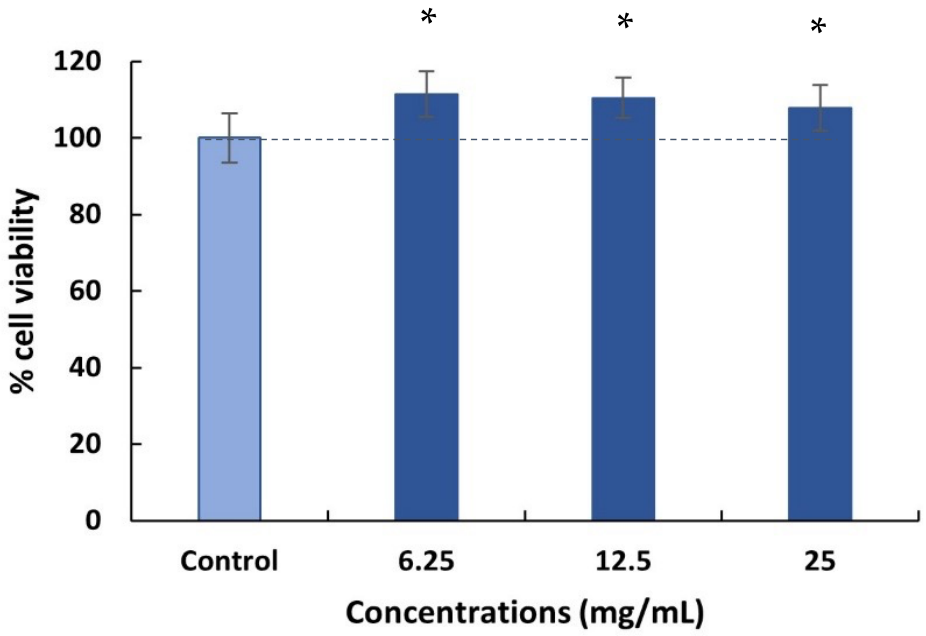

Figure 8. Percent cell viability of Res/GA-IC@hydrogels on NHF cells. (*Significant difference compared to control $p<0.05$)

While the *in vitro* results were promising, this study has several limitations that must be addressed. The long-term degradation behavior of the hydrogel *in vivo* was not assessed. Future studies must evaluate the degradation rate and its byproducts in a physiological environment. Furthermore, while the 24-h cytotoxicity assay showed excellent biocompatibility, long-term safety and the potential for any localized irritation or immune response over extended application periods must be investigated. These steps are crucial for the clinical translation of this platform. The need for *in vivo* efficacy testing, as previously mentioned, remains the most critical next step.

4. Conclusions

This study presents the innovative development of a dual-crosslinked PVA-CMC hydrogel patch incorporating Res/GA-IC for advanced wound care applications. The primary innovation of this work was the successful co-complexation and delivery of Res and GA, a combination shown here to possess strong quantifiable synergistic antioxidant activity (CI < 0.3). By co-encapsulating these agents in an HP-β-CD IC, we strategically overcame their significant aqueous solubility limitations and demonstrated enhanced antimicrobial efficacy against *S. aureus*. Integration of Res/GA-IC into a dual-network hydrogel matrix resulted in a bioactive dressing with favorable physicochemical characteristics, sustained release behavior, and excellent biocompatibility. The combined use of cyclodextrin-based complexation and hydrogel technology offers a novel and effective platform for delivering poorly soluble bioactive in wound care. It is important to note that this study focused on the *in vitro* formulation, characterization, and proof-of-concept. While these results are highly promising, the lack of *in vivo* validation is a limitation. Future preclinical studies in animal models are a necessary and warranted next step to confirm the translational potential of this hydrogel patch in a clinical setting. In summary, this work demonstrated a significant advancement in the design of multifunctional wound dressings by leveraging synergistic antioxidant effects and improved solubility through inclusion complexation. The developed hydrogel patch holds strong potential for future use in advanced wound management.

CRediT author statement

Khin Cho Aye: Methodology, Software, Formal analysis, Investigation, Writing - Original Draft. **Supusson Pengnam:** Validation, Data Curation. **Boonnada Pamornpathomkul:** Validation, Resources. **Thapakorn Charoenying:** Software, Data Curation. **Prasopchai Patrojanasophon:** Conceptualization, Visualization. **Praneet Opanasopit:** Conceptualization, Validation, Resources, Supervision, Project administration, Funding acquisition. **Chaiyakarn Pornpitchanarong:** Conceptualization, Methodology, Validation, Formal analysis, Writing - Review & Editing, Visualization, Supervision, Project administration.

Acknowledgement

This research was funded by Silpakorn University under the post-doctoral fellowship program. The authors gratefully acknowledge the Faculty of Pharmacy, Silpakorn University, for providing facilities and instrumental support.

Competing Interests

The authors state that there are no competing interests to declare.

References

1. Wang M, Deng Z, Guo Y, Xu P. Engineering functional natural polymer-based nanocomposite hydrogels for wound healing. *Nanoscale Adv.* 2022; 5(1): 27-45. doi:10.1039/d2na00700b
2. Gounden V, Singh M. Hydrogels and Wound Healing: Current and Future Prospects. *Gels.* 2024; 10(1). doi:10.3390/gels10010043
3. Sen CK. Human Wound and Its Burden: Updated 2022 Compendium of Estimates. *Adv Wound Care (New Rochelle).* 2023; 12(12): 657-70. doi:10.1089/wound.2023.0150
4. Koehler J, Brandl FP, Goepferich AM. Hydrogel wound dressings for bioactive treatment of acute and chronic wounds. *European Polymer Journal.* 2018; 100: 1-11. doi:10.1016/j.eurpolymj.2017.12.046
5. Op 't Veld RC, Walboomers XF, Jansen JA, Wagener F. Design Considerations for Hydrogel Wound Dressings: Strategic and Molecular Advances. *Tissue Eng Part B Rev.* 2020; 26(3): 230-48. doi:10.1089/ten.TEB.2019.0281
6. Tavakoli S, Klar AS. Advanced Hydrogels as Wound Dressings. *Biomolecules.* 2020; 10(8). doi:10.3390/biom10081169

7. Munusamy T, Shanmugam R. Enhancing wound healing with nanoparticle-infused hydrogels: a review of current applications and future prospects. *Discover Biotechnology.* 2025; 2(1): 34. doi:10.1007/s44340-025-00030-1
8. Nasibi S, Nargesi khoramabadi H, Arefian M, Hojjati M, Tajzad I, Mokhtarzade A*, et al.* A review of Polyvinyl alcohol / Carboxiy methyl cellulose (PVA/CMC) composites for various applications. *Journal of Composites and Compounds.* 2020; 2(3): 68-75. doi:10.29252/jcc.2.2.2
9. Capanema NSV, Mansur AAP, Carvalho IC, Carvalho SM, Mansur HS. Bioengineered Water-Responsive Carboxymethyl Cellulose/Poly(vinyl alcohol) Hydrogel Hybrids for Wound Dressing and Skin Tissue Engineering Applications. *Gels.* 2023; 9(2). doi:10.3390/gels9020166
10. Mansur AAP, Rodrigues MA, Capanema NSV, Carvalho SM, Gomes DA, Mansur HS. Functionalized bioadhesion-enhanced carboxymethyl cellulose/polyvinyl alcohol hybrid hydrogels for chronic wound dressing applications. *RSC Adv.* 2023; 13(19): 13156-68. doi:10.1039/d3ra01519j
11. Wang L-Y, Wang M-J. Removal of Heavy Metal Ions by Poly(vinyl alcohol) and Carboxymethyl Cellulose Composite Hydrogels Prepared by a Freeze–Thaw Method. *ACS Sustainable Chemistry & Engineering.* 2016; 4(5): 2830-7. doi:10.1021/acssuschemeng.6b00336
12. Chang C, Lue A, Zhang L. Effects of Crosslinking Methods on Structure and Properties of Cellulose/PVA Hydrogels. *Macromolecular Chemistry and Physics.* 2008; 209(12): 1266-73. doi:10.1002/macp.200800161
13. Raza A, Chohan TA, Zaidi SHH, Hai A, Alzahrani AR, Abida*, et al.* A Systematic Review on Biochemical Perspectives on Natural Products in Wound Healing: Exploring Phytochemicals in Tissue Repair and Scar Prevention. *Chemistry & Biodiversity.* 2024; 21(10): e202400615. doi:https://doi.org/10.1002/cbdv.202400615
14. Jia Y, Shao JH, Zhang KW, Zou ML, Teng YY, Tian F*, et al.* Emerging Effects of Resveratrol on Wound Healing: A Comprehensive Review. *Molecules.* 2022; 27(19). doi:10.3390/molecules27196736
15. Brumberg V, Astrelina T, Malivanova T, Samoilov A. Modern Wound Dressings: Hydrogel Dressings. *Biomedicines.* 2021; 9(9). doi:10.3390/biomedicines9091235
16. Badhani B, Sharma N, Kakkar R. Gallic acid: a versatile antioxidant with promising therapeutic and industrial applications. *RSC Advances.* 2015; 5(35): 27540-57. doi:10.1039/c5ra01911g
17. Gobin M, Proust R, Lack S, Duciel L, Des Courtils C, Pauthe E*, et al.* A Combination of the Natural Molecules Gallic Acid and Carvacrol Eradicates P. aeruginosa and S. aureus Mature Biofilms. *Int J Mol Sci.* 2022; 23(13). doi:10.3390/ijms23137118

18. Hao X, Sun X, Zhu H, Xie L, Wang X, Jiang N*, et al.* Hydroxypropyl-β-Cyclodextrin-Complexed Resveratrol Enhanced Antitumor Activity in a Cervical Cancer Model: In Vivo Analysis. *Frontiers in Pharmacology.* 2021; 12. doi:10.3389/fphar.2021.573909
19. Fan G, Yu Z, Tang J, Dai R, Xu Z. Preparation of gallic acid-hydroxypropyl-β-cyclodextrin inclusion compound and study on its effect mechanism on Escherichia coli in vitro. *Materials Express.* 2021; 11(5): 655-62. doi:10.1166/mex.2021.1968
20. Wangsawangrung N, Choipang C, Chaiarwut S, Ekabutr P, Suwantong O, Chuysinuan P*, et al.* Quercetin/Hydroxypropyl-beta-Cyclodextrin Inclusion Complex-Loaded Hydrogels for Accelerated Wound Healing. *Gels.* 2022; 8(9). doi:10.3390/gels8090573
21. Micale N, Citarella A, Molonia MS, Speciale A, Cimino F, Saija A*, et al.* Hydrogels for the Delivery of Plant-Derived (Poly)Phenols. *Molecules.* 2020; 25(14). doi:10.3390/molecules25143254
22. Aye KC, Rojanarata T, Ngawhirunpat T, Opanasopit P, Pornpitchanarong C, Patrojanasophon P. Development and optimization of curcumin-nanosuspensions with improved wound healing effect. *Journal of Drug Delivery Science and Technology.* 2023; 89: 104997. doi:https://doi.org/10.1016/j.jddst.2023.104997
23. Chou TC. Theoretical basis, experimental design, and computerized simulation of synergism and antagonism in drug combination studies. *Pharmacol Rev.* 2006; 58(3): 621-81. doi:10.1124/pr.58.3.10
24. pal singh M, Gupta A, Singh S. Qualitative Analysis of Gallic Acid by HPLC Method In Different Extracts of Terminalia Bellerica Roxb. Fruit Qualitative Analysis of Gallic Acid by HPLC Method In Different Extracts of Terminalia Bellerica Roxb. Fruit. *Fabad Journal of Pharmaceutical Sciences.* 2019; 44: 101-6.
25. Rosiak N, Cielecka-Piontek J, Skibinski R, Lewandowska K, Bednarski W, Zalewski P. Antioxidant Potential of Resveratrol as the Result of Radiation Exposition. *Antioxidants (Basel).* 2022; 11(11). doi:10.3390/antiox11112097
26. Thanyacharoen T, Chuysinuan P, Techasakul S, Nooeaid P, Ummartyotin S. Development of a gallic acid-loaded chitosan and polyvinyl alcohol hydrogel composite: Release characteristics and antioxidant activity. *Int J Biol Macromol.* 2018; 107(Pt A): 363-70. doi:10.1016/j.ijbiomac.2017.09.002
27. Vivero-Lopez M, Sparacino C, Quelle-Regaldie A, Sanchez L, Candal E, Barreiro-Iglesias A*, et al.* Pluronic(R)/casein micelles for ophthalmic delivery of resveratrol: In vitro, ex vivo, and in vivo tests. *Int J Pharm.* 2022; 628: 122281. doi:10.1016/j.ijpharm.2022.122281

28. Osamudiamen PM, Oluremi BB, Oderinlo OO, Aiyelaagbe OO. Trans-resveratrol, piceatannol and gallic acid: Potent polyphenols isolated from Mezoneuron benthamianum effective as anticaries, antioxidant and cytotoxic agents. *Scientific African.* 2020; 7. doi:10.1016/j.sciaf.2019.e00244
29. Shojaee MS, Moeenfard M, Farhoosh R. Kinetics and stoichiometry of gallic acid and methyl gallate in scavenging DPPH radical as affected by the reaction solvent. *Sci Rep.* 2022; 12(1): 8765. doi:10.1038/s41598-022-12803-3
30. Li Z, Chen X, Liu G, Li J, Zhang J, Cao Y*, et al.* Antioxidant Activity and Mechanism of Resveratrol and Polydatin Isolated from Mulberry (Morus alba L.). *Molecules.* 2021; 26(24). doi:10.3390/molecules26247574
31. Jensen GS, Wu X, Patterson KM, Barnes J, Carter SG, Scherwitz L*, et al.* In vitro and in vivo antioxidant and anti-inflammatory capacities of an antioxidant-rich fruit and berry juice blend. Results of a pilot and randomized, double-blinded, placebo-controlled, crossover study. *J Agric Food Chem.* 2008; 56(18): 8326-33. doi:10.1021/jf8016157
32. Carneiro SB, Costa Duarte FI, Heimfarth L, Siqueira Quintans JS, Quintans-Junior LJ, Veiga Junior VFD*, et al.* Cyclodextrin(-)Drug Inclusion Complexes: In Vivo and In Vitro Approaches. *Int J Mol Sci.* 2019; 20(3). doi:10.3390/ijms20030642
33. Li J, Xu F, Dai Y, Zhang J, Shi Y, Lai D*, et al.* A Review of Cyclodextrin Encapsulation and Intelligent Response for the Release of Curcumin. *Polymers (Basel).* 2022; 14(24). doi:10.3390/polym14245421
34. Christaki S, Spanidi E, Panagiotidou E, Athanasopoulou S, Kyriakoudi A, Mourtzinos I*, et al.* Cyclodextrins for the Delivery of Bioactive Compounds from Natural Sources: Medicinal, Food and Cosmetics Applications. *Pharmaceuticals (Basel).* 2023; 16(9). doi:10.3390/ph16091274
35. Lu Z, Cheng B, Hu Y, Zhang Y, Zou G. Complexation of resveratrol with cyclodextrins: Solubility and antioxidant activity. *Food Chemistry.* 2009; 113(1): 17-20. doi:https://doi.org/10.1016/j.foodchem.2008.04.042
36. Song Y, Huang H, He D, Yang M, Wang H, Zhang H*, et al.* Gallic Acid/2-Hydroxypropyl-β-cyclodextrin Inclusion Complexes Electrospun Nanofibrous Webs: Fast Dissolution, Improved Aqueous Solubility and Antioxidant Property of Gallic Acid. *Chemical Research in Chinese Universities.* 2021; 37(3): 450-5. doi:10.1007/s40242-021-0014-0
37. Radeva L, Yordanov Y, Spassova I, Kovacheva D, Tibi IP, Zaharieva MM*, et al.* Incorporation of Resveratrol-Hydroxypropyl-beta-Cyclodextrin Complexes into Hydrogel Formulation for Wound Treatment. *Gels.* 2024; 10(5). doi:10.3390/gels10050346

38. Yan M, Huang S, Li X, Wang Y, Zhong S, Ban J*, et al.* Gallic Acid Nanocrystal Hydrogel: A Novel Strategy for Promoting Wound Healing and Inhibiting Scar Formation. *Int J Nanomedicine.* 2025; 20: 4607-26. doi:10.2147/IJN.S514961
39. Ding J, Li X, Jin Z, Hachem MA, Bai Y. Efficient glycosylation of polyphenols via dynamic complexation of cyclodextrin and synchronous coupling reaction with cyclodextrin glycosyltransferase in water. *International Journal of Biological Macromolecules.* 2024; 280: 136065. doi:https://doi.org/10.1016/j.ijbiomac.2024.136065
40. dos Santos Lima B, Shanmugam S, de Souza Siqueira Quintans J, Quintans-Júnior LJ, de Souza Araújo AA. Inclusion complex with cyclodextrins enhances the bioavailability of flavonoid compounds: a systematic review. *Phytochemistry Reviews.* 2019; 18(5): 1337-59. doi:10.1007/s11101-019-09650-y
41. Suvarna V, Bore B, Bhawar C, Mallya R. Complexation of phytochemicals with cyclodextrins and their derivatives- an update. *Biomed Pharmacother.* 2022; 149: 112862. doi:10.1016/j.biopha.2022.112862
42. Kaleci B, Koyuturk M. Efficacy of resveratrol in the wound healing process by reducing oxidative stress and promoting fibroblast cell proliferation and migration. *Dermatologic Therapy.* 2020; 33(6): e14357. doi:https://doi.org/10.1111/dth.14357
43. Thi PL, Lee Y, Tran DL, Thi TTH, Kang JI, Park KM*, et al.* In situ forming and reactive oxygen species-scavenging gelatin hydrogels for enhancing wound healing efficacy. *Acta Biomater.* 2020; 103: 142-52. doi:10.1016/j.actbio.2019.12.009
44. Kowalczyk MC, Kowalczyk P, Tolstykh O, Hanausek M, Walaszek Z, Slaga TJ. Synergistic Effects of Combined Phytochemicals and Skin Cancer Prevention in SENCAR Mice. *Cancer Prevention Research.* 2010; 3(2): 170-8. doi:10.1158/1940-6207.Capr-09-0196
45. Hashemzaei M, Tabrizian K, Alizadeh Z, Pasandideh S, Rezaee R, Mamoulakis C*, et al.* Resveratrol, curcumin and gallic acid attenuate glyoxal-induced damage to rat renal cells. *Toxicol Rep.* 2020; 7: 1571-7. doi:10.1016/j.toxrep.2020.11.008
46. Kim JH, Lee BK, Lee KW, Lee HJ. Resveratrol counteracts gallic acid-induced down-regulation of gap-junction intercellular communication. *J Nutr Biochem.* 2009; 20(3): 149-54. doi:10.1016/j.jnutbio.2008.01.008
47. Liu J, Ma J, Wang Y, Hao H, Bi J, Hou H*, et al.* Synergistic Antibacterial Mechanism of Benzyl Isothiocyanate and Resveratrol Against Staphylococcus aureus Revealed by Transcriptomic Analysis and Their Application in Beef. *Foods.* 2025; 14(9). doi:10.3390/foods14091610

48. Wang XC, Huang HB, Gong W, He WY, Li X, Xu Y*, et al.* Resveratrol Triggered the Quick Self-Assembly of Gallic Acid into Therapeutic Hydrogels for Healing of Bacterially Infected Wounds. *Biomacromolecules.* 2022; 23(4): 1680-92. doi:10.1021/acs.biomac.1c01616
49. Duarte A, Martinho A, Luís Â, Figueiras A, Oleastro M, Domingues FC*, et al.* Resveratrol encapsulation with methyl-β-cyclodextrin for antibacterial and antioxidant delivery applications. *LWT - Food Science and Technology.* 2015; 63(2): 1254-60. doi:https://doi.org/10.1016/j.lwt.2015.04.004
50. Trinh XT, Long NV, Van Anh LT, Nga PT, Giang NN, Chien PN*, et al.* A Comprehensive Review of Natural Compounds for Wound Healing: Targeting Bioactivity Perspective. *Int J Mol Sci.* 2022; 23(17). doi:10.3390/ijms23179573
51. Shevelev AB, La Porta N, Isakova EP, Martens S, Biryukova YK, Belous AS*, et al.* In Vivo Antimicrobial and Wound-Healing Activity of Resveratrol, Dihydroquercetin, and Dihydromyricetin against Staphylococcus aureus, Pseudomonas aeruginosa, and Candida albicans. *Pathogens.* 2020; 9(4). doi:10.3390/pathogens9040296
52. Ghorpade VS, Yadav AV, Dias RJ, Mali KK, Pargaonkar SS, Shinde PV*, et al.* Citric acid crosslinked carboxymethylcellulose-poly(ethylene glycol) hydrogel films for delivery of poorly soluble drugs. *Int J Biol Macromol.* 2018; 118(Pt A): 783-91. doi:10.1016/j.ijbiomac.2018.06.142
53. Ghorpade VS, Dias RJ, Mali KK, Mulla SI. Citric acid crosslinked carboxymethylcellulose-polyvinyl alcohol hydrogel films for extended release of water soluble basic drugs. *Journal of Drug Delivery Science and Technology.* 2019; 52: 421-30. doi:10.1016/j.jddst.2019.05.013
54. Ouyang K, Zhuang J, Chen C, Wang X, Xu M, Xu Z. Gradient Diffusion Anisotropic Carboxymethyl Cellulose Hydrogels for Strain Sensors. *Biomacromolecules.* 2021; 22(12): 5033-41. doi:10.1021/acs.biomac.1c01003
55. Stauffer SR, Peppast NA. Poly(vinyl alcohol) hydrogels prepared by freezing-thawing cyclic processing. *Polymer.* 1992; 33(18): 3932-6. doi:https://doi.org/10.1016/0032-3861(92)90385-A
56. Ribeiro M, Simoes M, Vitorino C, Mascarenhas-Melo F. Hydrogels in Cutaneous Wound Healing: Insights into Characterization, Properties, Formulation and Therapeutic Potential. *Gels.* 2024; 10(3). doi:10.3390/gels10030188
57. Hassan CM, Peppas NA. Structure and Morphology of Freeze/Thawed PVA Hydrogels. *Macromolecules.* 2000; 33(7): 2472-9. doi:10.1021/ma9907587
58. Shin J-Y, Lee DY, Yoon JI, Song Y-S. Effect of CMC Concentration on Cell Growth Behavior of PVA/CMC Hydrogel. *Macromolecular Research.* 2020; 28(9): 813-9. doi:10.1007/s13233-020-8106-0

59. Wu S, Hua M, Alsaid Y, Du Y, Ma Y, Zhao Y*, et al.* Poly(vinyl alcohol) Hydrogels with Broad-Range Tunable Mechanical Properties via the Hofmeister Effect. *Advanced Materials.* 2021; 33(11): 2007829. doi:https://doi.org/10.1002/adma.202007829
60. Liu H, Chen L, Peng Y, Li X, Zhang H, Chen Y*, et al.* A tea polyphenol-loaded cellulose/silk fibroin/polyacrylic acid hydrogel for wound healing. *Cellulose.* 2024; 31(13): 8169-87. doi:10.1007/s10570-024-06102-5
61. Liang X, Zhong HJ, Ding H, Yu B, Ma X, Liu X*, et al.* Polyvinyl Alcohol (PVA)-Based Hydrogels: Recent Progress in Fabrication, Properties, and Multifunctional Applications. *Polymers (Basel).* 2024; 16(19). doi:10.3390/polym16192755
62. Tummala GK, Joffre T, Rojas R, Persson C, Mihranyan A. Strain-induced stiffening of nanocellulose-reinforced poly(vinyl alcohol) hydrogels mimicking collagenous soft tissues. *Soft Matter.* 2017; 13(21): 3936-45. doi:10.1039/C7SM00677B
63. Afni N, Taba P, Hala Y. Effect of carboxymethyl cellulose (CMC) concentration on water absorption on polyvinyl alcohol (PVA) hydrogels. *AIP Conference Proceedings.* 2023; 2588(1): 020008. doi:10.1063/5.0115925
64. Guan Y, Shao L, Dong D, Wang F, Zhang Y, Wang Y. Bio-inspired natural polyphenol cross-linking poly(vinyl alcohol) films with strong integrated strength and toughness. *RSC Advances.* 2016; 6(74): 69966-72. doi:10.1039/c6ra08904f
65. Li Z, Chen Z, Chen H, Chen K, Tao W, Ouyang XK*, et al.* Polyphenol-based hydrogels: Pyramid evolution from crosslinked structures to biomedical applications and the reverse design. *Bioact Mater.* 2022; 17: 49-70. doi:10.1016/j.bioactmat.2022.01.038
66. El-Sherbiny IM, Yacoub MH. Hydrogel scaffolds for tissue engineering: Progress and challenges. *Glob Cardiol Sci Pract.* 2013; 2013(3): 316-42. doi:10.5339/gcsp.2013.38
67. Huang X, Sun J, Chen G, Niu C, Wang Y, Zhao C*, et al.* Resveratrol Promotes Diabetic Wound Healing via SIRT1-FOXO1-c-Myc Signaling Pathway-Mediated Angiogenesis. *Front Pharmacol.* 2019; 10: 421. doi:10.3389/fphar.2019.00421
68. Yang DJ, Moh SH, Son DH, You S, Kinyua AW, Ko CM*, et al.* Gallic Acid Promotes Wound Healing in Normal and Hyperglucidic Conditions. *Molecules.* 2016; 21(7). doi:10.3390/molecules21070899
69. Mariello M, Binetti E, Todaro MT, Qualtieri A, Brunetti V, Siciliano P*, et al.* Eco-Friendly Production of Polyvinyl Alcohol/Carboxymethyl Cellulose Wound Healing Dressing Containing Sericin. *Gels.* 2024; 10(6). doi:10.3390/gels10060412